0273-2289/92/3435—0487$02.40

The One-Dimensional Biocatalyst

A Research Tool for *In Situ* Analysis of Immobilized-Cell Biocatalysts

R. M. WORDEN* AND L. G. BERRY

Department of Chemical Engineering, Michigan State University, East Lansing, MI 48824-1226

ABSTRACT

A new method to culture and analyze cells entrapped in porous gels has been developed that enables the properties of living, immobilized cells to be measured *in situ* as a function of depth within the gel. The method employs scanning fluorescence microscopy, which can provide rapid, sensitive, noninvasive measurements with a resolution of <1 mn. Any chemical species or cellular component that can be fluorescently marked can, in principle, be studied using this technique. Two applications of the approach are illustrated: measurement of transient diffusion rates within calcium alginate gel and monitoring growth of immobilized *Escherichia coli* cells.

INTRODUCTION

The importance of immobilized-cell bioprocesses to the biotechnology industry is well established, with applications including production of fuels, chemicals, pharmaceuticals, and diagnostics, as well as biological waste treatment (*1–5*). Immobilized-cell fermentations offer several advantages over comparable suspended-cell fermentations. By retaining cells in the reactor, product separation is simplified. The extremely high cell concentrations possible via immobilization result in high bioreactor productivities. Also immobilization has been known to have a desirable

*Author to whom all correspondence and reprint requests should be addressed.

effect on specific growth and product-formation rates, product yields, and plasmid stability (*6–17*).

The mechanisms by which immobilization affects cellular phenomena are not well understood. Consequently, attempts to model and design immobilized-cell bioprocesses mathematically have, in many cases, been unsatisfactory (*18–24*). One of the key factors involved is the mass-transfer resistance associated with the catalyst matrix and the immobilized cells. This resistance causes spatial gradients in substrate and product concentrations, and, as a result, gradients in other variables, including the concentration of viable cells and the physiological state of the cells.

Research efforts to elucidate immobilized-cell phenomena have been hampered by a lack of suitable analytical techniques. Ideally, such methods should be rapid, noninvasive, and possess a high spatial resolution to detect gradients within the biocatalyst. Standard optical methods, such as phase-contrast and fluorescence microscopy, can provide most of these capabilities. However, the outer region of the biocatalyst imposes a barrier to light that prevents examination of the inner regions without sectioning the sample. Other noninvasive methods, such as nuclear magnetic resonance spectroscopy, lack the speed and resolution of the optical methods.

Fluorescence has been used effectively to study immobilized cells. Doran and Bailey (*25*) used fluorescence spectroscopy to monitor NADH levels within immobilized *S. cerevisiae* cells. Cells were adsorbed onto strips of gelatin, attached to the wall of a curve, and loaded into a fluorescence spectrophotometer. Oscillations in NADH concentrations were observed, reflecting oscillatory trends frequently seen in continuous ethanol fermentations. This method illustrates the utility of fluorescence to monitor cellular dynamics, but lacks the spatial resolution needed to elucidate intraparticle gradients.

Scanning microfluorimetry was used to investigate the spatial gradient of RNA within spherical biocatalyst beads by Monbouquette and Ollis (*26*). Biocatalyst particles were removed from the reactor, and quickly chilled, fixed, sliced, and stained. Pyronin fluorescence was measured at 10-μm intervals across the radius of the bead to indicate the relative RNA concentrations. The relative cell concentration was also estimated from the proportions of cross-sectional area occupied by cell mass and void space, respectively. This approach shows the capabilities of scanning fluorescence microscopy to elucidate gradients within porous biocatalysts, but it requires the cells to be killed. Thus, cellular dynamics could not be directly measured with this method.

We have developed a new analytical approach that couples scanning fluorescence microscopy with a novel biocatalyst configuration (the One-Dimensional Biocatalyst, or ODB) to study living, immobilized cells *in situ*. The method is versatile, in that any cellular component for which there is a fluorescent marker can, in principle, be studied. In addition, gradients in the desired variables can be measured with respect to both time and

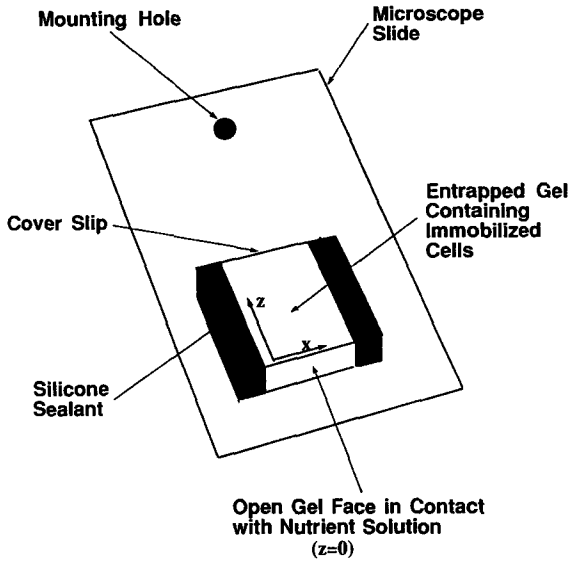

Fig. 1. Schematic diagram of One-Dimensional Biocatalyst.

position within the biocatalyst. The purpose of this article is to describe the method and to illustrate two of its applications: measurement of diffusion rates within the biocatalyst matrix and monitoring *Escherichia coli* growth within a calcium alginate gel.

METHODS

The ODB is shown schematically in Fig. 1. It consists of a thin slab of porous gel matrix encased within a sleeve made of glass or quartz. The ODBs were constructed from standard 20-mm square glass coverslips and 3×1 microscope slides. A hole was predrilled in one end of the slides for mounting in the bioreactor. A stainless-steel spacer maintained a 0.3-mm gap between the slide and coverslip while the sides were sealed with silicone glue. The ODB casings were steam-sterilized prior to being loaded with gel.

The gel is exposed to nutrient medium only along the open face (i.e., where $z=0$). Nutrients diffuse into the gel and are consumed by cells entrapped within. The simultaneous diffusion and chemical reaction phenomena can lead to concentration gradients in a number of chemical species, such as substrates, products, and oxygen. Additional gradients may also develop in biological variables, such as cell concentration, growth rate, RNA concentration, and so on. Because such gradients also occur within spherical, immobilized-cell biocatalysts, the ODB is the conceptual equivalent of a thin slice cut out of a spherical biocatalyst. However, unlike spherical biocatalysts, the geometry of the ODB facilitates a wide range of

in situ, microscopic and spectroscopic assays. Measurements taken along the *z*-direction of the ODB would correspond to measurements made at different depths within spherical biocatalysts. In addition, since fluorescence (and other optical) assays are available that do not interfere with cell metabolism, measurements on living cells with respect to both time and position are possible using scanning fluorescence microscopy.

The fluorescent stains, 6-carboxyfluorescein (CF) and 6-carboxyfluorescein (CFDA), were used for the diffusion and cell-growth studies, respectively. The CFDA is not fluorescent until its acetyl residues are cleaved by intracellular esterase enzymes to yield the highly fluorescent CF. Because of its very low background fluorescence and specificity for intracellular enzymes, CFDA makes an excellent marker for cell growth within the ODB. The peak wavelengths for excitation and emission of CF are 488 and 515 nm, respectively.

To study cellular properties as a function of depth within the biocatalyst using fluorescent stains, the location of the gel edge (i.e., $z=0$) must be known. However, when a fluorescent stain is used, the edge may not be apparent, because both the stain within the gel and that in the liquid fluoresce. To overcome this problem, fluorescein-conjugated latex microspheres 4 μm in diameter (FluoroSpheres, obtained from Molecular Probes, Inc., Eugene, OR) were added to the stain prior to its application to the gel. Thus, when using a concentration of soluble stain that fluoresces less intensely than the beads, the gel edge is clearly delineated by the sharp break in fluorescence intensity.

The following procedure was used to measure the diffusion rate of CF within the gel in the absence of cells. A 10 μg/mL CF aqueous solution was prepared from a 1 mg/mL stock solution in dimethyl sulfoxide (DMSO). A tracer stock solution containing 0.4 μL FluoroSpheres/mL water was also prepared. To initiate diffusion of the CF, 20 μL of a working solution consisting of 1% tracer solution in 10 μg/mL CF were added to the gel edge.

To monitor development of an active cell layer in the calcium alginate, ODBs were produced as described below. An inoculum culture of *Escherichia coli* cells (strain HB101, obtained from Pat Oriel, Michigan State University) was grown to an optical density (600 nm) of 0.9 in a 250-mL Erlenmeyer flask with a foam stopper. The flask was maintained at 37°C and in a water bath with 200 rpm shaking. The Luria Bertani (LB) medium contained (per liter): 10 g/L tryptone, 5 g/L yeast extract, and 5 g/L NaCl; the medium was supplemented with 10 m*M* $CaCl_2$, and the pH was adjusted to 7.2 prior to sterilization. The cells in 30 mL of the inoculum culture were recovered via centrifugation, resuspended in 1 mL of sterile water, and mixed into a suspension of 0.1 g $CaHPO_4$ in 25 mL of 3% (w/w) aqueous sodium alginate (low density, Sigma Chemicals). For ODB blanks, 1 mL of sterile water was added instead of the cell suspension. The internal gelation process (27) was initiated by the addition of 2.75 mL of 10% (w/v) D-gluconic acid lactone. The liquid gel was then quickly injected into the

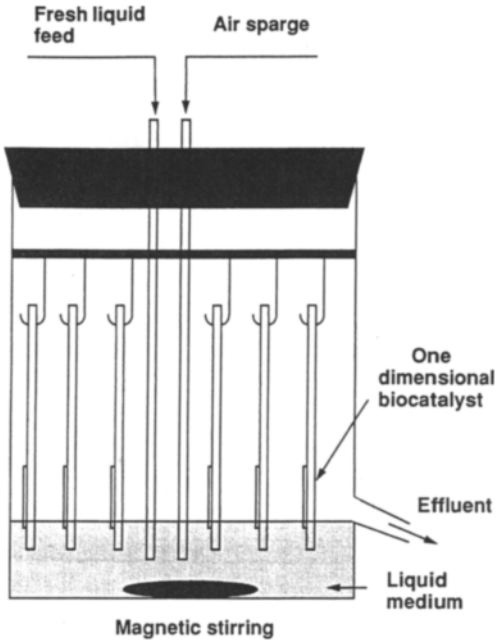

Fig. 2. Continuous bioreactor for ODB incubation.

ODB sleeves using a sterile syringe and 30-gage needle, and allowed to harden at room temperature for about an hour. Any excess gel protruding from the sleeve was sliced off with a sterile razor blade, and the ODBs were mounted in the reactor with their open gel faces submerged in the growth medium.

The continuous bioreactor used to develop the ODBs is shown schematically in Fig. 2. The vessel, constructed from a 2-L Pyrex graduated cylinder, was designed to be a stirred-tank reactor with a minimal liquid volume. This feature allows high dilution rates to wash out cells escaping from the gel quickly without requiring excessive volumes of medium. The liquid volume was 120 mL. The reactor has the capability for automatic control of pH, oxygen, and temperature, although, in these experiments, only the temperature was controlled at 37°C. Aerobic conditions were maintained by an air sparge. Liquid mixing was provided by magnetic stirring, and the temperature control system of a New Brunswick Multigen fermenter console (New Brunswick Scientific Co. Inc., Edison, NJ) was used to maintain the liquid temperature at 37°C. A dilution rate of 2.5 h^{-1} was used. At time intervals of 4 h, 2 ODBs were removed from the reactor and refrigerated at 4°C to stop cell growth. The experiment was continued over a 16-h period, after which the ODBs were transported at 4°C to another laboratory for analysis.

To detect *E. coli* cells, 20 μL of 20 μg/mL aqueous CFDA solution, prepared from a 1 mg/mL stock solution in DMSO, were added to the open

gel face. No fluorescent tracer beads were needed in this experiment. The stain only fluoresces after entering the cell and being cleaved by intracellular esterases. Thus, there is a clear demarcation between the nonfluorescent liquid phase and the fluorescent gel phase.

An ACAS 570 (Meridian Instruments, Okemos, MI) was used for the analyses. The ACAS consists of a computer-integrated microscope with micropositioning stage, a laser, and a photomultiplier. The microprocessor-controlled stage rapidly transports the sample past the microscope objective using selectable step sizes down to 0.25 μm. The sample is illuminated by the laser at preselected intervals. The resulting fluorescence emission is collected by the microscope objective, passed through optical filters, and measured with a sensitive photomultiplier. Data are recorded for later analysis and also displayed on a high-resolution, enhanced-graphics color monitor. Computer-aided image-analysis capabilities are used for data processing.

All ODBs were brought to room temperature before being run on the ACAS. Twenty microliters of the appropriate stain preparation were pipeted onto the open gel face to initiate the analysis. An arbitrary area of 300 μM wide (x dimension) by 1800 μm in the direction normal to the open gel face (z dimension) was scanned for fluorescence every 30 s, for 15 min. A Perkin Elmer Lambda 3A UV/visible spectrophotometer was used to measure the optical density of the alginate gel and cell suspensions.

RESULTS

Spectral Properties of the Gel

The spectral properties of the gel used in the ODB are important, because the gel must transmit UV and/or visible light. For a path length of 0.3 m, a 2% calcium alginate gel was found to adsorb about 1% of the incident light at 500 nm and about 3% at 350 nm. The fluorescein derivatives used in this study have excitation and emission maxima around 488 and 515 nm, respectively. Thus, absorbance of light by the gel was assumed to be negligible in these studies.

Measurement of Stain Diffusion Rates Within the ODB

Fluorescence profiles depicting the diffusion of CF into the gel are given in Fig. 3. The ordinate represents fluorescence intensity, and the abscissa gives distance along the z axis in micrometers. Each of the overlapping curves has two parts: the gel phase (right side) and the adjacent liquid phase (left side). All of the profiles within the gel originate from approximately the same point, which corresponds to the liquid-phase concentration of CF at the gel interface. To the left of this point, the fluo-

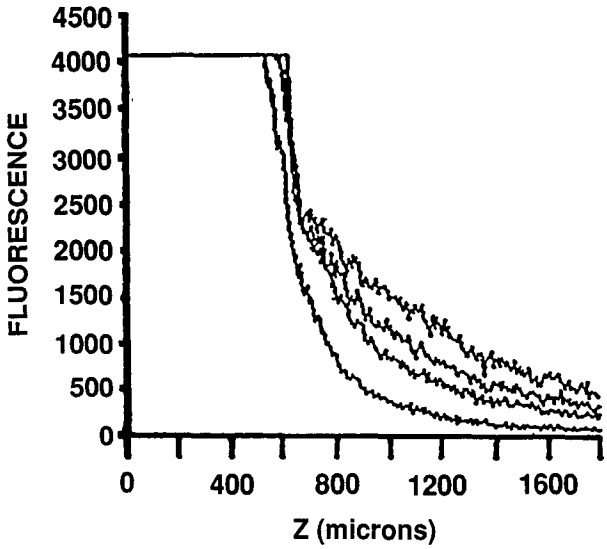

Fig. 3. Experimental fluorescence profiles within ODB: (a) 3 s, (b) 30 s, (c) 60 s, (d) 120 s.

rescence rises rapidly off the scale owing to the intense fluorescence of the FluoroSpheres. Thus, these graphs show that the tracer particles do effectively mark the gel–liquid interface. As time progresses, the CF wavefront progresses into the gel in a consistent pattern.

The geometry of the ODB was designed such that transport of a dissolved species into the gel would be well characterized by a one-dimensional (slab) transport model. The equation for the mass flux of the stain (N_A) in the water (B), relative to stationary coordinates is

$$N_A = X_A (N_A + N_B) - D_{AB} (dC_A / dz) \quad (1)$$

where X_A is the mass fraction of A, N_B is the mass flux of water, D_{AB} is the molecular diffusivity of the stain in water, C_A is the mass concentration of the stain at any point in the gel, and z is the spatial dimension, typically chosen to be the depth into the gel from the open face. For the very small concentrations of stain used in these experiments, Eq. 1 reduces to

$$N_A = - D_{AB} dC_A / dz \quad (2)$$

This equation may be substituted into an unsteady-state, one-dimensional mass balance on A within the gel to yield Fick's Second Law.

$$(\partial C_A / \partial t) = D_{AB} (\partial^2 C_A / \partial z^2) \quad (3)$$

The appropriate initial and boundary conditions would be

$$t = 0 \quad C_A = 0 \quad 0 \leq z < \infty$$
$$t > 0 \quad C_A = C_{A,0} \quad z = 0$$
$$t > 0 \quad C_A = 0 \quad z = \infty$$

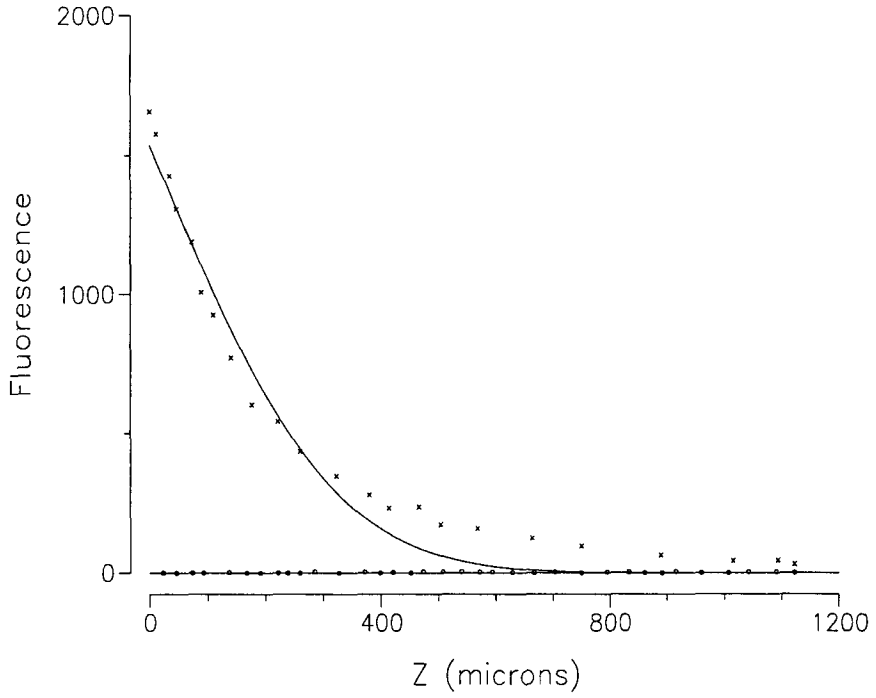

Fig. 4. Theoretical concentration profiles within ODB. O $t = 0$ s, x $t = 3$ s, — theroetical.

were $C_{A,0}$ is the concentration of A at the gel–liquid interface. The analytical solution is (*28*)

$$C_A = C_{A,0} \text{ erfc } [z / (4D_{AB}t)^{1/2}] \quad (4)$$

To illustrate that the experimentally measured profiles are consistent with those predicted by the one-dimensional diffusion model, examples of the transient concentration profiles predicted by the model are given in Fig. 4.

Monitoring Cell Growth Within Immobilized Cell Biocatalysts

Image scans taken 15 min after the application of CFDA to the open gel face are given in Fig. 5 for two incubation times: 0 h and 16 h. Because CFDA does not fluoresce until its acetyl pendant groups are cleaved, the fluorescence of the early samples with low cell densities is negligible. However, after several hours of cell growth, the fluorescence levels dramatically increase. The increase in cell densities predicted by the fluorescence measurements was confirmed qualitatively by visual and microscopic observation.

Quantitative representations of the data shown in Fig. 5, as well as data for intermediate time periods, are given in Fig. 6. These line scans

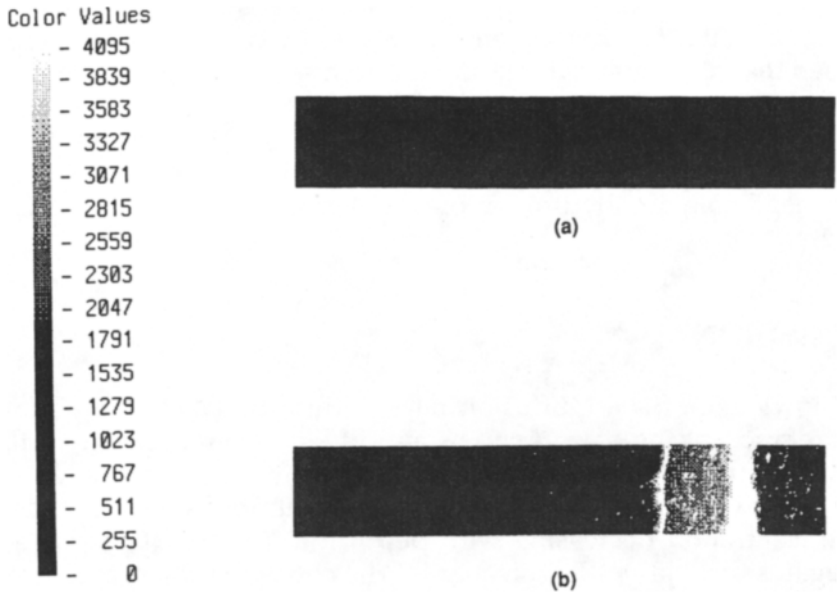

Fig. 5. Image-scans of CFDA fluorescence within ODB: (a) 0 h, (b) 16 h.

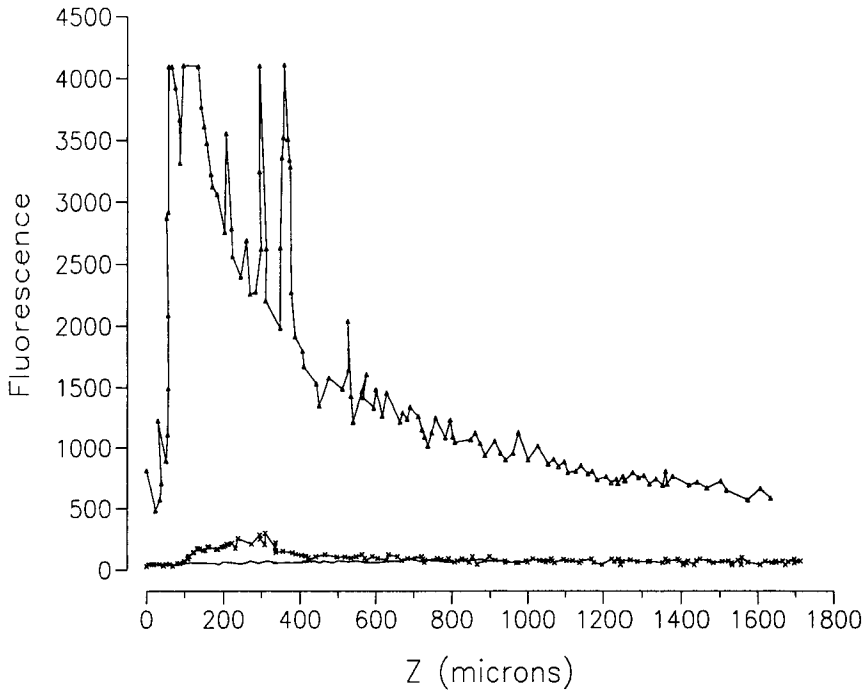

Fig. 6. CFDA fluorescence profiles within ODB. — $t=0$ h, X—X t=8 h, △—△ t=16 h.

correspond to the fluorescence levels taken across the z dimension at a constant x value. The fluorescence increases by two orders of magnitude between the initial-time sample and the 16-h sample, presumably because of the increased cell concentration. The fluorescence is highest near the edge of the gel and diminishes with increasing distance from the edge. The fluorescence level in the liquid phase maintains a very low level, indicating negligible autohydrolysis of CFDA and back-diffusion of CF into the liquid.

DISCUSSION

Knowledge of stain diffusion rates within the ODB is important for interpretation of the data. As the stain diffuses from the edge of the gel inward through the interstitial space, a transient concentration profile, or wave front, develops, with the highest concentrations near the edge and the concentration decreasing with depth into the gel. This wave front propagates through in the direction of the concentration gradient. When cells are also present in the gel, there could be additional gradients in cell properties (e.g., cell concentration). If the stain happens to be a selective indicator of one of these properties, then the two gradients will be superimposed, and it would be difficult to distinguish between them. However, this task would be simplified if the rate of stain transport were accurately characterized. Such information would be useful, both for planning experimental protocols and for estimating the impact of diffusion effects on the experimental results.

The results in Fig. 3 clearly illustrate that this technique has sufficient resolution and speed of response to track the stain's progression through the gel. The experimental concentration profiles show identical trends to the theoretical predictions given in Fig. 4. Thus, this approach appears suitable for measurement of molecular diffusivities of fluorescent stains in the gels. We are now developing such a method, based on identifying the value of the D_{AB} that minimizes the difference between the predicted profiles and those measured experimentally. Unsteady-state diffusion experiments have proven useful for determining molecular diffusivities of substrates within alginate gel spheres (*29,30*). However, this approach is apparently novel. Additionally, it could be applied equally well to gels containing entrapped cells.

The results shown in Figs. 5 and 6 are consistent with the visually observed growth of cells within the gel. The fluorescence increases by two orders of magnitude between the inoculum and 16-h ODBs, and the fluorescence intensity is highest near the gel–liquid interface. The fluorescent intensity has not yet been correlated with viable cell density within the ODB, and quantitative interpretation of these data is expected to be difficult. As described above, the fluorescence intensity at a particular time and location in the gel is a function of both the rate of stain diffusion

and the concentration of cells (and/or some property of the cells). Also, if there are dynamics associated with the production of fluorescing molecules once the cell encounters the stain, as may be the case with CFDA, an additional complication is introduced. Thus, research may be needed to calibrate the dynamics of each stain used. An alternative method of staining, in which the coverslip is temporarily removed and the stain is applied uniformly to the top of the gel slab, is also under investigation. This method would allow the stain to be instantaneously applied in identical concentrations to all points along the z axis.

The image scans depicting diffusion of CF (data not shown) were smoother and more uniform in the y direction than those depicting cell growth (e.g., Fig. 5b). In some cases, the latter image scans showed local regions of high intensity, having dimensions on the order of 10–20 μm. These fluctuations are thought to be the result of nonuniform growth of cells within the gel. Cellular growth as microcolonies, rather than as a homogeneous dispersion, has been observed by others (*31*). We have also observed a fragmentation of the gel surface, as evidenced by a ragged gel-liquid interface, after about 15 h of growth (data not shown). The disruption of the gel is thought to be the result of excessive growth. This phenomenon is commonly observed for microbial growth in polysaccharide gels.

This study has demonstrated the use of the One-Dimensional Biocatalyst to study immobilized cell biocatalysts. The combination of the ODB geometry and a sophisticated scanning fluorescence microscope, such as the ACAS 570, yields a research tool with enormous power and versatility. The method can, in principle, measure any chemical species or cellular component for which fluorescent stains are available, and make such measurements as a function of both position and time within the biocatalyst. The method has sufficient resolution to measure fluorescence of individual cells, sufficient speed to measure transient diffusion through the gel matrix, and the extreme detection sensitivity inherent to fluorescence. Because the method is also noninvasive, the cells can be examined *in situ*, with minimal, or negligible, disturbance of their environment and activity. Thus, cellular dynamics of entrapped cells may be measured under conditions simulating those in actual bioreactors. Research is under way to refine further the techniques presented here and to demonstrate other applications of the method. Information obtained using this approach could dramatically improve the understanding of immobilized-cell behavior, and thereby improve the accuracy of mathematical models and design calculations for immobilized-cell bioprocesses.

ACKNOWLEDGMENTS

This material is based upon work supported by the National Science Foundation under Grant No. BCS-8909840. The government has certain rights in this material.

REFERENCES

1. Scott, C. D. (1987), *Enz. and Microb. Tech.* **9,** 66.
2. Fukui, S. and Tanaka, A. (1982), *Ann. Rev. Microbiol.* **36,** 145.
3. Chibata, I., Tosa, T., and Fujimura, M. (1983), *Annual Reports on Fermentation Processes,* vol. 6, Academic, New York, 1.
4. Borglum, B. G. and Marshall, J. J. (1984), *Appl. Biochem. and Biotech.* **9,** 117.
5. Blanch, H. W. (1984), *Annual Reports on Fermentation Processes,* vol. 7, Academic, New York, p. 81.
6. Furaske, S., Seki, M., and Fukumura, K. (1983), *Biotech. and Bioeng.* **25,** 2921.
7. Alleman, J. E., Viel, J. A., and Canaday, J. T. (1982), *Water Res.* **16,** 543.
8. Burrill, H. B., Bell, L., Greenfield, P. F., and Do, D. D. (1983), *Appl. and Environ. Microbiol.* **46,** 716.
9. Fletcher, M. (1986), *Appl. and Env. Micro.* **52,** 672.
10. Tyagi, R. D. and Ghose, T. K. (1982), *Biotech. and Bioeng.* **24,** 781.
11. Kjelleberg, S., Humphrey, B. A., and Marshall, K. C. (1982), *Appl. and Envir. Micro.* **43,** 1166.
12. Kirchman, D. and Mitchell, R. (1982), *Appl. and Envir. Micro.* **43,** 200.
13. Hattori, R. (1972), *J. Gen. Appl. Microbiol.* **18,** 319.
14. Marin-Iniesta, F., Nasri, M., Dhulster, P., Barbotin, J., and Thomas, D. (1988), *Appl. Microb. Biotechnol.* **28,** 455.
15. Marin-Iniesta, F., DeTaxis du Poet, P., Dhulster, P., Thomas, D., and Barbotin, J. (1987), *Ann. N.Y. Acad. Sci.* **501,** 317.
16. Oriel, P. (1988), *Enz. and Microb. Tech.* **10,** 517.
17. Bailey, K., Wieth, W. R., and Chotani, G. K. (1987), *Ann. N.Y. Sci.* **506,** 196.
18. Benefield, L. and Molz, F. (1983), *Biotech. and Bioeng.* **25,** 2591.
19. Benefield, L. and Molz, F. (1985), *Biotech. and Bioeng.* **27,** 921.
20. Andrews, G. F. (1982), *Biotech. and Bioeng.* **26,** 2013.
21. Park, Y., Davis, M. E., and Wallis, D. A. (1984), *Biotech. and Bioeng.* **26,** p. 457.
22. Tang, W. T. and Fan, L. S. (1985), Steady State Phenol Biodegradation in a Draft Tube Gas-Liquid-Solid Fluidized Bed Bioreactor," paper presented at 190th ACS National Meeting, Chicago, IL, September 8–14.
23. Mellick, M. R., Karim, M. N., Linde, B. E., Dale, B. E., and Mihaltz, P. (1986), *Biotech. and Bioeng.* **29,** 370.
24. Park, Y., Davs, M. E., and Wallis, D. A. (1984), *Biotech. and Bioeng.* **26,** 468.
25. Doran, P. M. and Bailey, J. E. (1987), *Biotech. and Bioeng.* **29,** 892.
26. Monbouquette, H. F. and Ollis, D. F. (1988), *Bio/Techhnology* **6,** 1076.
27. Johansen, A. and Flink, J. M. (1986), *Biotech. Letters,* **8,** 121.
28. Bird, R. B., Stewart, W. E., and Lightfoot, E. N. (1960), *Transport Phenomena,* John Wiley, New York, p. 125
29. Hannoun, B. J. M. and Stephanopoulos, G. (1986), *Biotech. and Bioeng.* **28,** 829.
30. Petersen, J. N., Davison, B. H., and Scott, C. D. (1991), *Biotech. and Bioeng.* **37,** 386.
31. Monbouquette, H. G. and Ollis, D. F. (1990), *Frontiers in Bioprocessing,* Sikdar, S. K., Bier, M., and Todd, P., eds., CRC, Baca Raton, FL, p. 65.